Indian Journal of Chemical Technology
Vol. 29, November, 2022 pp. 678-687
DOI: 10.56042/ijct.v29i6.67400

*p*H and temperature dual-sensitive molecular imprint polymers for BSA based on Cu^{2+} coordination

Xiangzhi Dong[1,2], Baoliang Zhang[2] & Qiuyu Zhang*[,2]

[1]Key Laboratory of Applied Physics and Chemistry in Space of Ministry of Education, School of Natural and Applied Sciences, Northwestern Polytechnical University, Youyi Road 127#, Xi′an 710 072, China

[2]College of Environmental and Chemical Engineering, Xi′an Polytechnic University, Jinhua Nan Road 19#, Xi′an 710 048, China

E-mail: dongxz6566@foxmail.com

Received 19 August 2022; Accepted 21 October 2022

A novel kind of pH and temperature dual-sensitive Molecular imprint polymers (MIPs) combined with Cu^{2+} coordination (SiO_2@CS/NIPAM-Cu^{2+}-MIP) has been synthesized using glycidyl methacrylate-iminodiacetic acid (GMA-IDA) as a metal chelating ligand, with bovine serum albumin (BSA) as template protein, combined with *p*NIPAM and chiston (CS) as temperature and *p*H sensitive monomers, respectively. The coordination effect of GMA-IDA-Cu^{2+} has been shown to be beneficial to improve the adsorption capacity and adsorption specificity of BSA. The influence of *p*H not only changed the charge force between the polymer and protein in the imprinting system, but also deformed the imprinting cavity through the protonation of NH_3^+ on CS. Further, the thermo-sensitivity of the imprinted polymer was also found to be satisfactory. With the joint efforts of coordination, electrostatic action and good matching of imprinted sites, higher adsorption capacity (173.48 $mg \cdot g^{-1}$) and imprinting factor (2.72) have been obtained at *p*H 4.6 and 35ºC. Although it took about 4 h to reach saturation adsorption, the cyclability of the SiO_2@CS/NIPAM-Cu^{2+}-MIP was found to be acceptable and the adsorption capacity was maintained at original 81.16% after six cycles. It is for the first time that GMA-IDA-Cu^{2+} has been used to prepare the *p*H and temperature dual-sensitive imprinted polymer for BSA.

Keywords: GMA-IDA-Cu^{2+}, Molecular imprinting polymer, *p*H and temperature dual-sensitivity

Inspired by the biosystem of antigen-antibody, artificial molecular imprint polymers (MIPs) have been successfully designed to have an intelligent controllably adsorbing and releasing specific compound by using molecular imprinting technique (MIT)[1-5]. The preparation process and action principle of MIPs revealed that firstly, templates had been polymerized with appropriate functional monomers and cross-linking agents, and then the template had been eluted. The resulting materials contained tailor-made recognition sites potentially complementary to templates in shape and size comparable with those of natural receptors. Due to the reversibility of this "specific binding", MIPs were very attractive and have been applied in wide areas[6-9]. However, most of the research on MIPs is related to small molecules because there are lots of challenges which hindered the development of macromolecular imprinting. For proteins, large volume structure, flexible molecular conformation and complex surface are the obstacles to the improvement of adsorption and recognition performances, nevertheless the efforts of the researchers[10-13].

In order to overcome the imprinting difficulties caused by the intrinsic characteristics of proteins, many imprinting strategies have been proposed. For example, water-soluble monomers and mild imprinting conditions were used to avoid protein denaturation. In addition, surface imprinting was often adopted to reduce the mass transfer resistance of macromolecules. For example, epitope technology with corresponding feature fragment combined with surface imprinting was usually used to reduce mass transfer resistance. Yang *et al.*[14] used the N-terminal peptides of serum albumin, immunoglobulin G and transderrin, as the epitope templates, the multiepitope templates imprinted particles were formed through self-assembly with poly (ether sulfone). The obtained imprinted particles can simultaneous identify three target proteins in human plasma with high selectivity at the same time. Zhang *et al.*[15] used C-terminus nonapeptide of bovine serum albumin (BSA) as a model epitope, synthesized an oriented surface epitope-imprinted open-mouthed polymer nanocapsules (OM-MIP NCs) by sacrificing asymmetric template-modified Janus nanocores.

Although researchers explored some appropriate strategies, more efforts should be committed to improve the adsorption efficiency and rebinding specificity simultaneously. In recent years, development of environmental responsive MIPs had been focused, which capable of changing their physicochemical properties or morphologies in response to external stimuli (temperature, *p*H, light and so on)[16-25]. Poly(N-isopropylacrylamide) (PNIPAM) was used as the temperature-sensitive monomer to prepare temperature sensitive MIPs so as to exhibit the reversible expanded/collapsed conformational transition at the lower critical solution temperature (LCST). Zhang *et al.*[16] accomplished MIPs with BSA as protein template and NIPAM as temperature-sensitive monomer onto the surface of hollow Fe_3O_4 microspheres, the fabricated BSA-imprinted microspheres had excellent adsorption capacity under the optimal temperature 32ºC. Wu *et al.*[26] synthesized opto-thermally responsive molecularly imprinted membranes (OT-MIMs) by using NIPAM as thermally backbone monomer and Au as the light-heat converters, the maximum adsorption capacity of OT-MIMs was obtained at 35ºC.

In addition, *p*H-sensitivility protein MIPs were another notable subject. The responsive behavior achieved owed to *p*H-sensitive monomers, which always contained cationic groups such as amino and pyridine groups or anionic groups such as carboxyl groups, can be protonation or deprotonation at different *p*H, resulting in shrinked or expanded of MIPs system. Chitosan is a natural polysaccharide with good biocompatibility and contains both amino and carboxyl groups, which can be used as an amphoteric *p*H sensitive monomer[27,28].

Besides, metal ions can form chelates with proteins which contain naked histidine, and this effect has no specificity and ignoring the structure and morphology of proteins[29-32]. Therefore, researchers combined metal coordination with proteins molecularly imprinted technology to prepare imprinting materials with specificity recognition and higher imprinting efficiency. Qin *et al.*[33] prepared temperature-sensitive imprinted hydrogel for Lyz using N-(4-vinyl)-benzyl iminodiacctic acid (VBIDA) as ligand and Cu^{2+} as coordination, the obtained imprinting material showed higher selectivity, compared with those which were which prepared without VBIDA-Cu^{2+}. Li *et al.*[34] used GMA-IDA-Cu^{2+} to prepare the temperature sensitive imprinting polymers, strikingly highly imprinting factor (up to 22.7) had exhibited.

Based on the previous works, in this paper, GMA-IDA-Cu^{2+} had been employed as the metal chelating ligands and grafted on the surface of nano-SiO_2, combined with temperature sensitive monomer NIPAM and pH sensitive monomer CS, BSA had been choosed as template protein, after imprinted copolymerization with functional monomer MAA and crosslinker MBA, a *p*H and temperature dual-sensitive MIPs were prepared, and the binding properties were investigated subsequently.

Experimental Section

Materials and Reagents

Tetraethyl silicate (TEOS), tetramethylethylene-diamine (TEMED), ammonium persulfate (APS), methacrylic acid (MAA), glycidyl methacrylate (GMA), chitosan (CS), iminodiacetic acid (IDA), N,N-methylene-bisacrylamide (MBA), cerium ammonium nitrate (CAN), copper sulfate pentahydrate ($CuSO_4 \cdot 5H_2O$), sodium dodecyl sulfate (SDS),ethylene diamine tetraacetic acid (EDTA) were purchased from Sinopharm Chemical Reagent Co., Ltd. N-isopropyl-acrylamide (NIPAM), γ-(2,3-epoxypropoxy) propyl-trimethoxysilane (GPTMS) were obtained from Aladdin Reagent Co., Ltd. Bovine serum albumin (BSA), Human serum albumin (HSA), Ovalbumin (OVA), Bovine hemoglobin (BHb), lysozyme (Lyz), and trypsin (Tryp) were acquired from Shanghai Lanji Technology development Co., Ltd. Other reagents were all analytical pure and can be used directly. NIPAM was recrystallized with n-hexane before use.

Characterization

The morphology of the polymers was observed by JEOL JEM-2100 Plus transmission electron microscope (TEM, Japan Electronics Co., Ltd., Japan) and FLEXSEM 1000 (SEM, Hitachi, Japan). TG/TGA 851^e thermogravimetric analyzer (TGA, Mettler-Toledo, Switzerland) and Nicolet-5700 Infrared Spectrometer (IR, Thermo-Fisher, USA) were used to test the functional groups and composition of the polymers, respectively. The concentration of proteins in supernatant was measured by UV 2450 spectro-photometer (UV, Shimadzu, Japan).

Synthesis of *p*H and temperature dual-sensitive imprinted polymers with metal coordination

Synthesis of GMA-IDA

GMA-IDA monomer was synthesized by the ring opening reaction between epoxy group of GMA

monomer and IDA. IDA was neutralized with NaOH to form sodium iminodiacetate (IDA-2Na^+) to avoid the reaction of carboxylate in IDA with epoxy group. The IDA-2Na^+ solution was slowly added into GMA monomer (the molar ratio is 1:1), and the clarified product was obtained by mix the solution vigorously at 60°C for 2 h.

Perparation of SiO_2@GMA-IDA

The preparation of monodisperse SiO_2 was synthesized by the Stöber method as described in our previous work[35]. The obtained SiO_2 redistributed and the pH was adjusted to 4.0-4.5 using oxalic acid, then 4 mL of GPTMS was added dropwise, and the reaction continued for 24 h, and the final product GPTMS modified SiO_2 (SiO_2-GPTMS) was obtained after washed repeatedly by ethanol and water.

Then, the epoxy group of GPTMS-SiO_2 was hydrolyzed to diol by added 100 mL 0.5M H_2SO_4 and stirred at 90°C for 2 h. After washing to neutral, the product was added into 100 mL phosphoric acid buffer (PBS, *p*H = 7.0), and the reaction was carried out at 60°C for in N_2 atmosphere, and the reaction was allowed to continue for 4 h after adding 5 mL GMA-IDA monomer. The final SiO_2@GMA-IDA was obtained by repeatedly washing with deionized water.

Perparation of pH and temperature dual-sensitive imprinted polymers with metal coordination

Chitosan solution 0.5% (w/v) was prepared with 100 mL acetic acid for standby. 300 mg of SiO_2@GMA-IDA and 0.0113 mmoL $CuSO_4{\cdot}5H_2O$ were mixed in 10 mL of 0.02 M PBS solution and stirred for 2 h to fully coordinate Cu^{2+} with IDA. Then the solution was incubated with BSA (30 mg) for another 1 h. After that, added 20 mL PBS buffer containing 1 mmol NIPAM, 0.5 mmol MBA, 2 mmol MAA, and 1 mmol CAN, mixed with 10 mL chitosan acetic acid solution, and stirred for 2 h to complete prepolymerization. The polymerization reaction was initiated by injected 10 mg APS and 10 μL TEMED, and continued for 24 h at 35°C. In order to avoid other side reactions caused by oxygen, all polymerization reactions were carried out in nitrogen atmosphere.

The obtained polymerization MIPs were eluted repeatedly with EDTA solution (0.1 M), NaCl (0.5M), 10% (v/v) acetic acid solution contained 10% SDS (w/v)and deionized water to remove template and unreacted monomers, until the eluate was detected to be unabsorbed at the wavelength of 278 nm. Then, the particles were incubated in $CuSO_4$ solution (0.1 M) for 30 min to reloaded Cu^{2+}. Finally, the obtained MIPs, labeled as SiO_2@CS/NIPAM-Cu^{2+}-MIPs, were washed extensively with deionized water and dried for further use. In addition, non imprinted polymers (SiO_2@CS/NIPAM-Cu^{2+}-NIPs) were also prepared similarly except for the absence of template protein BSA.

Meanwhile, in order to verify the effect of metal chelating ligand GMA-IDA-Cu^{2+} in imprinting recognition, polymers without GMA-IDA-Cu^{2+} were prepared by the same method, and named as SiO_2@CS/NIPAM-MIP and SiO_2@CS/NIPAM-NIP, respectively.

Protein rebinding experiments

Saturated adsorption capacity, adsorption kinetics, specificity and repeatability are main indexes to evaluate the performance of imprinted polymer.

About 10 mg of SiO_2@CS/NIPAM-Cu^{2+}-MIPs were incubated with 5 mL 0.6 mg·mL^{-1} template protein solution for 24 h at 35°C, and then centrifuged. The concentration of template protein in the supernatant was detected by ultraviolet spectroscopy at 278 nm. The adsorption capacity of imprinted polymers to template protein was calculated as follows:

$$Q = \frac{(C_0 - C)V}{m} \quad \ldots (1)$$

where Q was the adsorption capacity of imprinted polymers to template protein (mg·g^{-1}), C_0 was the initial concentration of BSA solution (mg·mL^{-1}), C was the equilibrium concentration of of BSA in the supernatant after adsorption (mg·mL^{-1}), respectively, V was the volume of BSA solution (mL), and m was the mass of imprinted polymers (g).

Imprinting factor (IF) and selective factor (β) were calculated by the following formula to evaluate the specificity recognition properties of imprinted polymers:

$$IF = \frac{Q_{MIP}}{Q_{NIP}} \quad \ldots (2)$$

$$\beta = \frac{IF_{tem}}{IF_{com}} \quad \ldots (3)$$

where Q_{MIP} and Q_{NIP} were the adsorption capacity of MIP and NIP, IF_{tem} and IF_{com} were the imprinting factor of template protein and competitive protein, respectively.

Results and Discussion

Fabrication of SiO_2@CS/NIPAM-Cu^{2+}-MIPs

The chelation between metal ions and proteins can be used to improve the imprinting efficiency of MIPs on proteins with naked histidine on the surface.

Ligands containing amion or alcohol groups at both the ends, one end combined with carriers and the other end formed strong chelation with metal ions to fix them. In this paper, iminodiacetic acid (IDA) was chosen for some advantages as following. First, IDA occupied three empty orbitals of the transition metal, and the remaining empty orbital domain can form a strong coordination with proteins. Second, IDA is a straight chain structure and the smallest ligand, the resistance was least when binding to proteins. Third, the non-specific adsorption can be effectively reduced because the polymers were electric neutral after coordination with metal ions, attributed to the hydrophilicity and electro negativity of IDA[36-38]. Figure 1 illustrates the preparation process of SiO_2@ CS/NIPAM-Cu^{2+}-MIPs.Cu^{2+} had been coordinated with GMA-IDA which had been fabricated on the SiO_2, then the template protein BSA was chelated with Cu^{2+}. Subsequently, in the presence of *p*H sensitive monomer CS and temperature sensitive monomer NIPAM, combined with other monomers, the *p*H and temperature dual-sensitive MIPs were fabricated.

Characterization

The typical morphologies of SiO_2,SiO_2-GMA-IDA,SiO_2@CS/NIPAM-Cu^{2+}-MIP and SiO_2@CS/ NIPAM-Cu^{2+}-NIP had been shown in Fig. 2. All the materials had good dispersion, and the carrier SiO_2 were regular spherical with smoothly surface (Fig. 2a). After grafting, the surface of SiO_2-GMA-IDA began to rough obviously, indicating that ligand GMA-IDA had been grafted successfully (Fig. 2b). The surface smoothness ofSiO_2@CS/NIPAM-Cu^{2+}-MIP and SiO_2@CS/NIPAM-Cu^{2+}-NIP changed again, attributed to the coating of the imprinted layer. And the TEM images of both can be clearly observed that the outer layer was wrapped with an imprinted layer (Fig. 2(c and 2d inset).

The FTIR diagrams of SiO_2(A), SiO_2@GMA-IDA(B), SiO_2@CS/NIPAM-Cu^{2+}-MIPs(C)and SiO_2

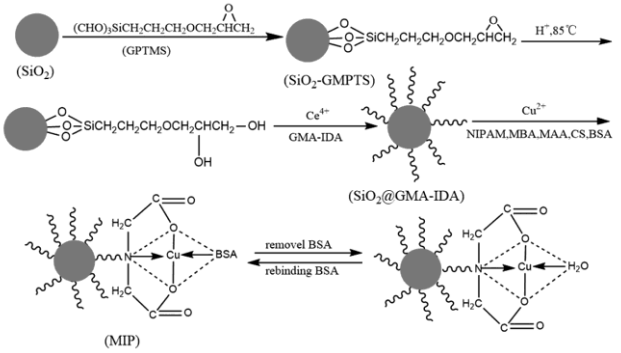

Fig. 1 — Preparation of *p*H and temperature dual-sensitive imprinted polymers with metal coordination

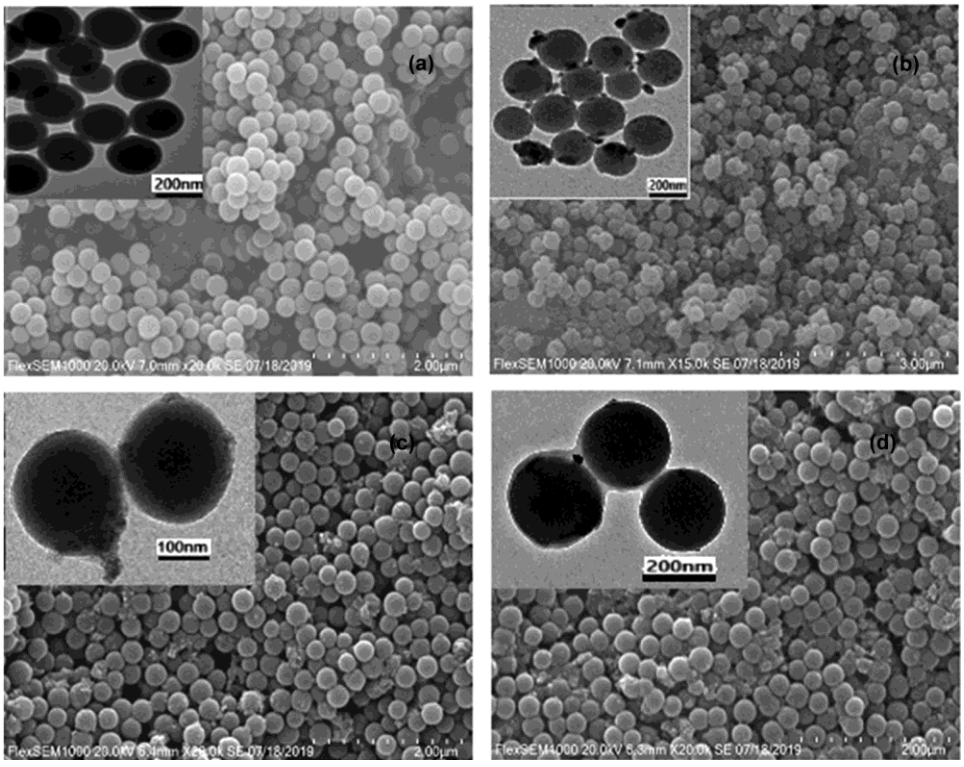

Fig. 2 — SEM and TEM images of (a) SiO_2 ; (b) SiO_2-GMA-IDA; (c) SiO_2@CS/NIPAM-Cu^{2+}-MIP and (d) SiO_2@CS/NIPAM-Cu^{2+}-NIP

@CS/NIPAM-Cu^{2+}-NIP(D) were showed in Fig. 3(a). Among them, 1105 cm^{-1}, 804 cm^{-1} and 470 cm^{-1} were the characteristic peaks of SiO_2, and the wide peak of -OH at 3400 cm^{-1} indicates that SiO_2 has good hydrophilicity. After grafted, the peak at 1700-1400 cm^{-1} were broaden, caused by the stretching vibration of COO- symmetry and anti-symmetry in GMA-IDA monomer. For SiO_2@CS/NIPAM-Cu^{2+}-MIP and SiO_2@CS/NIPAM-Cu^{2+}-NIP, the peak at 1650 cm^{-1} were increased and sharper due to superposition of the absorption peak of amide group in NIPAM. The C-H peaks at 2922 cm^{-1} and 2854 cm^{-1} indicate that the imprinted polymers had been successfully prepared.

Figure 3(b) showed the thermo-gravimetric curves, which can evaluate the outer polymer contents of nanoparticles to a certain extent.SiO_2 had almost no thermal weight loss. After grafted, the weight loss of SiO_2@GMA-IDA was about 30% for the decomposed GMA-IDA. Combined with IR spectrum, it was proved that GMA-IDA had been successfully grafted.

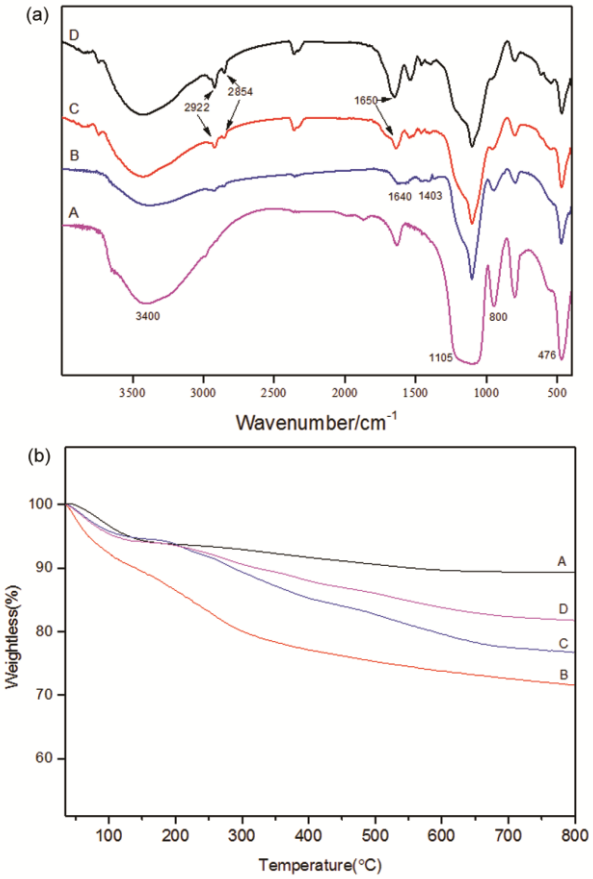

Fig. 3 — (a) FTIR spectrograms and (b) thermogravimetric diagrams of SiO_2 (A), SiO_2@GMA-IDA (B), SiO_2@CS/NIPAM-Cu^{2+}-MIP(C) and SiO_2@CS/NIPAM-Cu^{2+}-NIP (D)

However, the weight loss rates of SiO_2@CS/NIPAM-Cu^{2+}-MIPs and SiO_2@CS/NIPAM-Cu^{2+}-NIP were decreased compared with SiO_2@GMA-IDA, were 23.27% and 18.24%, respectively. That was because the degree of cross linking in the imprinted layer increased after imprinting polymerization, which made the heat resistance increased.

_p_H and temperature dual-sensitivity of imprinted polymers

Based on the previous experimental results[39-44], the adsorption capacity Q and *IF* of the polymers were investigated at different conditions: between 20°C to 40°C, and *p*H 4.6-8.0, to evaluate the *p*H and temperature dual-sensitivity of imprinted polymers.

*p*H will not only affect the charge property of the protein, but also affect the amino protonation on the CS chains in the imprinted layer and then affect the shape of the imprinted cavity. And these changes will affect the binding force between the imprinted sites and the template proteins, resulting in the change of adsorption capacity. In view of the thermo-sensitive property of *p*NIPAM, the influence of *p*H was investigated at two typical temperatures, 35°C and 25°C. Firstly, BSA solution with a concentration of 0.8 $mg \cdot mL^{-1}$ was prepared with buffer at *p*H 4.6, 6.0, 7.0, 8.0, respectively. Then, 5 mL of above BSA solution and 10 mg of imprinted polymers were placed in the centrifuge tube, shaken and then adsorbed for 4 h until equilibrium. The *p*H sensitivity of imprinted polymers was evaluated by the adsorption capacity as shown in Fig. 4(a).

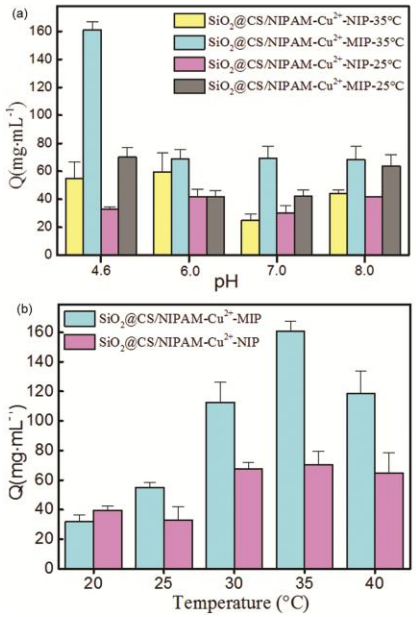

Fig. 4 — Effect of *p*H and temperature on the adsorption capacities of imprinted polymers

In general, regardless of the temperature, the adsorption capacity of SiO_2@CS/NIPAM-Cu^{2+}-MIPs at *p*H 4.6 was much higher than other *p*H conditions. At *p*H 4.6, the steric resistance can be minimized for the imprinted cavity expanded, which caused by the charge repulsion from the -NH_2 s received protons to form -NH_3^+on the CS main chain. Meanwhile, the electrostatic force increased because the ligand GMA-IDA-Cu^{2+} was electro-negative and BSA had a small amount of positive charge, the BSA could be bounded easily under these double effects. The adsorption capacity decreased sharply when pH increased to 6.0, which was the result of two synergistic effects: (I) the steric resistance increased by the imprinted cavity shrunk, which caused by the deprotonation of -NH_3^+changed to -NH_2 on the CS chains; (II) the ligand and BSA were all negatively charged made the electrostatic repulsion increased, so the combination was difficult. And these two forces continuously affect the adsorption capacity of the imprinted polymers with the increased of *p*H, resulting the lower adsorption capacities at alkaline *p*H.

Owing to the absence of template protein during preparation of SiO_2@CS/NIPAM-Cu^{2+}-NIP, the shape of imprinted cavities and the arrangement of functional groups were randomly. Then the effect of *p*H on the adsorption capacities was irregular, for the magnitudes of binding resistance as well as the effects of protonation and electrostatic interaction were also disordered. For all that, the maximum adsorption capacity of SiO_2@CS/NIPAM-Cu^{2+}-NIP was less than 60 $mg \cdot g^{-1}$, far below than the SiO_2@CS/NIPAM-Cu^{2+}-MIP under the same condition, which sufficiently proved the importance of imprinting shape and sites arrangement on the adsorption properties of imprinted polymers.

In addition, the adsorption capacities of the imprinted polymers at 35°C were all higher than 25°C, as shown in Fig. 4(a), indicating that the temperature also affect the adsorption performance. In order to study the thermo-sensitivity comprehensively, the adsorption capacities at 20, 30 and 40°C had been investigated. It should be noted that the *p*H of BSA solution was fixed at 4.6, and the imprinted cavities had been expanded by the protonation of CS chains at this time. It is well known that the pNIPAM chains shrink or stretch depending on the temperature, higher or lower, than LCST. In other words, the imprinted cavities and sites arrangement of the imprinted polymers would be affected by both *p*H and temperature. From the results shown in Fig. 4(b), the adsorption capacity was the smallest at 20°C due to the serious deformation of imprinted cavity and the imprinted sites were inconsistent with the template protein, which caused by the relaxation of *p*NIPAM chain combined with the swelling of CS, the binding between proteins and imprinted cavities was weakly. The adsorption capacity increased with the increased of temperature, benefited by the reconstruction of imprinted cavities and the recovery of binding ability with BSA, which triggered by the shrinkage of pNIPAM chains. When the temperature reached 35°C, which was also the preparation temperature, the adsorption capacity was maximum, indicated that the imprinting cavity and site arrangement were the most matched with the template protein. However, the adsorption capacity decreased again with the further increased of temperature, for the excessive contraction of the imprinted cavity leaded to the weakening of the binding force with the template protein. For SiO_2@CS/NIPAM-Cu^{2+}-NIPs, the adsorption performance was also affected by temperature, and the adsorption capacity was smaller by the lack of specific internal imprinting sites.

The above results confirmed that the imprinted polymer had good *p*H and temperature dual-sensitivity and the recognition mechanism had been shown in the Fig. 5 below. The imprinted polymer shrank too much at high temperature and high *p*H, and swelled too much at low temperature and low *p*H. Then, the imprinted cavity and sites deformed violently, which was not conducive to the binding of template protein. The shape of imprinted cavity was restored only under suitable conditions (*p*H 4.6 and 35°C), and the strong coordination effect of metal Cu^{2+} on template protein obtained a large adsorption capacity.

Metal coordination effects

The adsorption capacity of proteins which has naked histidine can be increased by inclusion of metal ions[42-44]. Therefore, we also prepared MIPs with different metal ions, defined as SiO_2@CS/NIPAM-***x***-MIPs (***x*** represents metal ions, ***n*** means no metal ions), to compare the effects of metal coordination on the adsorption properties of BSA. From Fig. 6, the adsorption capacity of SiO_2@CS/NIPAM-***n***-MIPs was lower than that of SiO_2@CS/NIPAM-***x***-MIPs, which proved that the coordination between proteins and metal ions was more effective than other non-covalent interactions. Then, the metal coordination effects on protein imprinted materials were analyzed. The ability of different metal ions to BSA decreased in the order

of Cu^{2+}>Fe^{2+}>Ni^{2+}>Zn^{2+}>Mn^{2+}, and Cu^{2+} displayed the best BSA-coordination ability (Q=160.36 mg g^{-1}, IF=2.20), followed by Fe^{2+} (Q=111.57 mg g^{-1}, IF=1.65). It was noticed thatSiO_2@CS/NIPAM-Mn^{2+}-MIPs had good IF for BSA, indicted that Mn^{2+} has excellent biocompatibility, which had been proved in the previous works[45,46]. In sum, metal coordination was favorable for enhancing imprinting performances.

Adsorption properties of imprinted polymers

Binding isotherm

Firstly, 10 mg of SiO_2@CS/NIPAM-Cu^{2+}-MIP was added into BSA solution with initial concentration of 0.1-1.0 mg·mL^{-1} to adsorb until equilibrium, and the relationship between initial concentration and saturated adsorption capacity had been drawn in Fig. 7(a). It can be seen that the adsorption capacity of SiO_2@CS/NIPAM-Cu^{2+}-MIP increased with the increase of concentration of BSA initially, indicated that BSA in solution had being bound to the adsorption sites. Then, the adsorption capacity tended to be stable above 0.6 mg·mL^{-1}, speculated that the imprinting site had been completely generated and the adsorption was saturated basically.

However, the adsorption curve of SiO_2@CS/NIPAM-Cu^{2+}-NIP was relatively flat and almost saturated at 0.3 mg·mL^{-1}, for there were no imprinting sites. Finally, 0.8 mg·mL^{-1} was selected concentration for the follow-up experiment, because both the adsorption capacity and the imprinting factor were all satisfactory, which were 173.48 mg·mL^{-1} and 2.72, respectively. The adsorption was fitted by Langmuir equation as given in Equation (4).

$$\frac{C_e}{Q} = \frac{C_e}{Q_{max}} + \frac{1}{KQ_{max}} \quad \ldots (4)$$

where, Q and Q_{max} represent the experimental adsorption capacity and theoretical maximum adsorption capacity (mg·g^{-1}), *Ce* is the concentration of protein in the equilibrium solution (mg·mL^{-1}), K is the Langmuir adsorption equilibrium constant. Table 1 listed the estimated values and imprinted factors, together with those obtained from SiO_2@CS/NIPAM-MIP and SiO_2@CS/NIPAM-NIP for the purpose of comparison. The correlations of Langmuir curve of these polymers were good, means the adsorption model of BSA belongs to monolayer adsorption. The constant K represents the affinity of MIP to template, higher K indicates stronger affinity. The value of K and Q_{max} of SiO_2@CS/NIPAM-Cu^{2+}-MIP were all bigger than SiO_2@CS/NIPAM-Cu^{2+}-NIP, means that the adsorption ability of SiO_2@CS/NIPAM-Cu^{2+}-MIP

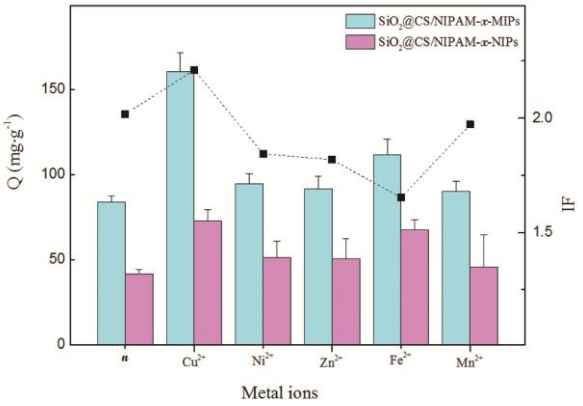

Fig. 6 — Effect of metalions on the adsorption capacities of imprinted polymers

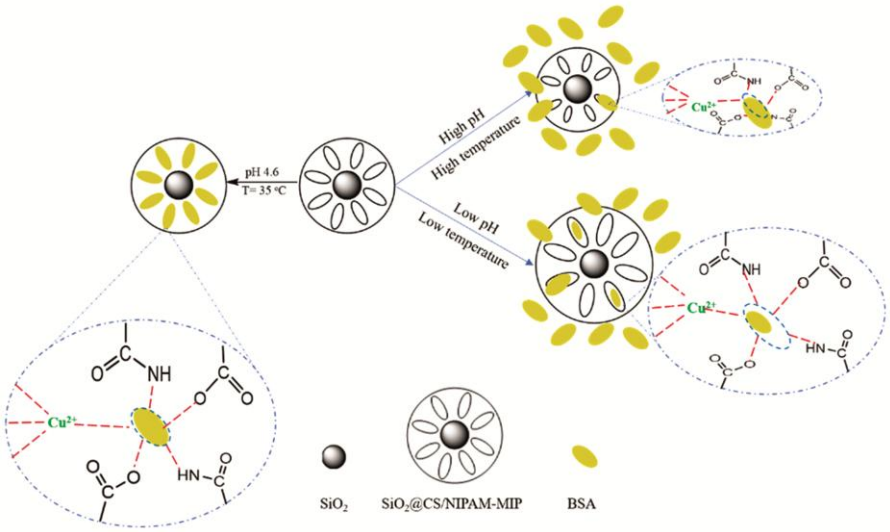

Fig. 5 — Schematic diagram of the process of protein adsoprption through volume phase change (swelling/shrinking) caused by the change of temperature and *p*H

were excellent. The value of *K* and *IF* of SiO_2@CS/NIPAM-Cu^{2+}-MIP were greater than those of SiO_2@CS/NIPAM-MIP, indicated that the coordination can not only increase the adsorption capacity, but also improve the specific adsorption of template protein.

Binding kinetics

The adsorption kinetics of imprinted polymers were investigated under the optimal adsorption conditions, and the adsorption kinetics was shown in Fig. 7 (b). The adsorption capacity of SiO_2@CS/NIPAM-Cu^{2+}-MIP was increased rapidly at first, for the template protein bound to the sites under the electrostatic, hydrogen and chelating force. After 4 h, the growth rate slowed down to reach equilibrium. However, the adsorption equilibrium time of SiO_2@CS/NIPAM-Cu^{2+}-NIP was shorter, for there were no recognition sites and cavities to interact with BSA.

Rebinding specificity and stability

Five different proteins, BHb, HSA, OVA, Lyz and Tryp, were chosen as references to evaluate the specific recognition performance of imprinted polymers, and the results were listed in Table 2. It is worth mentioning that all the proteins at pH 4.6, all competitive proteins were positively and the forces that determine the adsorption performance include electrostatic force, the recognition sites, the size of cavities and the coordination with GMA-IDA-Cu^{2+}.

There always have some naked histidine and tryptophan residues on the surface of protein, and the GMA-IDA-Cu^{2+} included in the imprinted polymers have strong coordination and binding ability with them[47-49]. Compared with BSA, BHb have similar molecular weight and higher pI, and the binding ability between BHb and Cu^{2+} was strong, as there are 15 tryptophans on its surface. However, the adsorption capacity of MIP to BHb is not high, as the BHb is a kind of tetramer double concave protein composed of two different polypeptides, which has significant shape difference with the elliptical protein

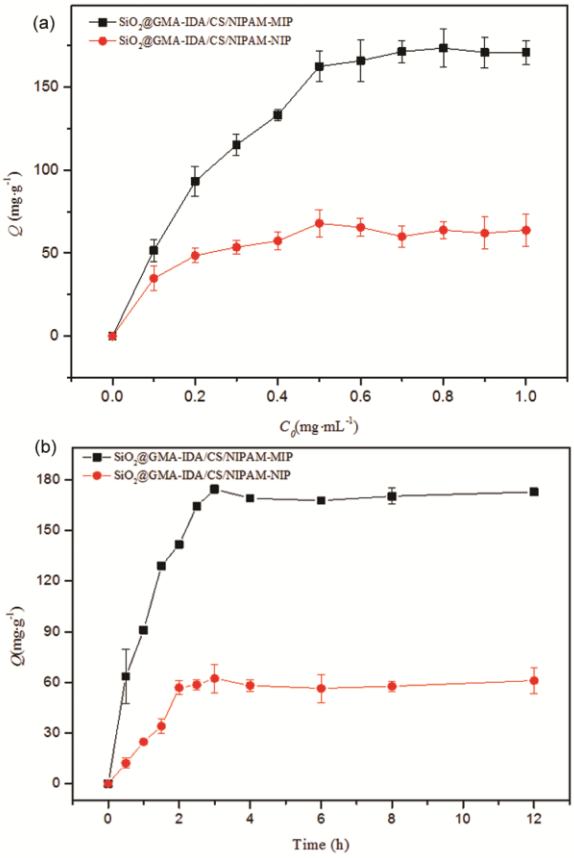

Fig. 7 — (a) Adsorption isotherm (b) andadsorption kinetics of BSA on SiO_2@CS/NIPAM-Cu^{2+}-MIP and SiO_2@CS/NIPAM-Cu^{2+}-NIP

Table 1 — Estimated values of Langmuir and imprinted factors

Samples	*Q*（mg·g^{-1}）	*K*(mL·mg^{-1})	*Qmax*(mg·g^{-1})	R^2	*IF*
SiO_2@CS/NIPAM-Cu^{2+}-MIP	173.48	33.14	179.73	0.9937	2.72
SiO_2@CS/NIPAM-Cu^{2+}-NIP	63.87	27.38	65.18	0.9932	-
SiO_2@CS/NIPAM-MIP	83.74	16.91	89.03	0.9969	2.02
SiO_2@CS/NIPAM-NIP	41.52	5.51	53.43	0.9825	-

Table 2 — The adsorption properties of SiO_2@CS/NIPAM-Cu^{2+}-MIP and SiO_2@CS/NIPAM-Cu^{2+}-NIP for different proteins

Proteins	Molecular Weight Mw(KDa)	Isoelectric Point PI	Adsorption capacityQ/mg·g^{-1}		IF	β
			MIP	NIP		
BSA	66	4.9	170.05	60.89	2.79	-
BHb	68	6.8	66.06	31.07	2.13	1.31
HSA	66	4.7-4.9	73.80	38.77	1.90	1.11
OVA	43	4.7	56.88	27.99	2.03	1.37
Lyz	14.3	11	53.02	33.47	1.58	1.76
Tryp	24	10.8	64.42	55.21	1.17	2.39

of BSA. Although it had been attracted to the cavity by metal coordination, the strong steric resistance effect prevents it from binding to the sites. The adsorption capacity of MIP to HSA was slightly greater than other competitive proteins. The speculated reason was that HSA have similar molecular weight, isoelectric point and amino acid residues with BSA (HSA has a free cysteine residue and BSA has two tryptophan residues), but smaller molecular size, so they can easily approach the imprinted sites under the coordination effect. Then, the electrostatic repulsion force caused by the inconsistent site arrangement will hinder the binding of protein, so the adsorption capacity was less than the template protein. The coordination between OVA and GMA-IDA-Cu^{2+} was weak and the molecular size of OVA does not match the imprinted cavity, so the binding rate was very low. And for Lyz, which could be approached to the imprinted sites and combined with them easily under the influence of coordination and electrostatic action, for which has smaller molecular weight and more positive charge. But the adsorption capacity was relatively low. That maybe because the imprinted cavity was not completely matched with it, and the binding force was weak too. Tryp was similar to this situation, and the coordination between Tryp and GMA-IDA-Cu^{2+} was not strong at pH 4.6, and hence failed to fetch high adsorption capacity.

According to the results of specific adsorption, the adsorption capacity of competitive proteins with large molecular weight was smaller than that of competitive proteins with small molecular weight. It means that the shape of imprinted cavity and site arrangement were the important factors to determine the

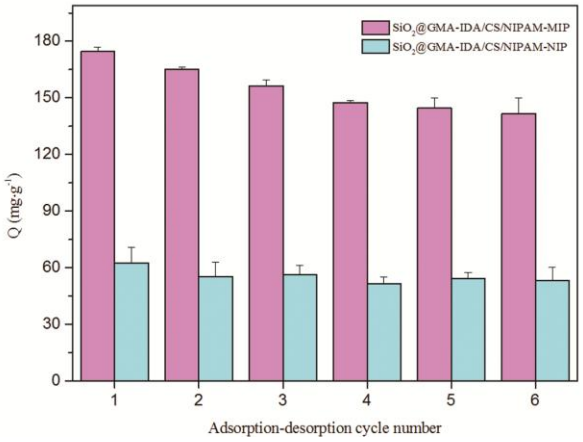

Fig. 8 — Recyclability of SiO_2@CS/NIPAM-Cu^{2+}-MIP and SiO_2@CS/NIPAM-Cu^{2+}-NIP

recognition performance of SiO_2@CS/NIPAM-Cu^{2+}-MIP, and the coordination of GMA-IDA-Cu^{2+} can increase the binding ability of template protein and site. The selective factor (β) also showed that the imprinted polymer had good specific recognition.

Recyclability is not only an important index to evaluate the performance of materials, but also an important index to evaluate the application potential of materials. The adsorption-elution cycle tests had been carried out by putting 10 mg of SiO_2@CS/NIPAM-Cu^{2+}-MIP into BSA solution (0.8 $mg \cdot mL^{-1}$), and the results were showed in Fig. 8. It can be found that the adsorption performance of SiO_2@CS/NIPAM-Cu^{2+}-MIP reduced gradually. The possible reason was that the strong binding force between GMA-IDA-Cu^{2+} and protein, and a large number of eluents were needed in each cycle to completely remove the binding template protein. Thus, the imprinted cavity and site had been damaged inevitable. The change of the adsorption capacity of SiO_2@CS/NIPAM-Cu^{2+}-NIP was irregularly for there have no suitable imprinting cavities and the binding sites, and some functional groups which were favorable for binding with BSA may be exposed during the elution process. Even though, the adsorption capacity decreased by 18.84% after six cycles, and it was still considered to be a stable protein imprinting material.

Conclusion

In this paper, NIPAM and CS have been used as temperature and *p*H sensitive monomers respectively, combined with GMA-IDA-Cu^{2+} used as coordination agent to construct a protein molecularly imprinted polymer with high adsorption capacity and *p*H and temperature dual-sensitivity. Meanwhile, with the joint efforts of coordination, electrostatic action and good matching of imprinted sites, higher adsorption capacity and imprinting factor have been obtained. Although, the stability of the imprinted polymer is not so good, it is still a significant attempt to prepare *p*H and temperature dual-sensitivity MIP by combining metal coordination.

Acknowledgement

This study was supported by the State Key Program of the National Natural Science of China (No. 51433008), the National Natural Science Foundation of China (No. 21704084, 21975206 and 51873169), and the Shaanxi Innovative Talents Promotion Plan-the Young Star of Science and Technology Project (No. 2019KJXX-67), National

Natural Science Foundation of Shaanxi (No. 2018JM2028) and the Fundamental Research Funds for the Central Universities (No. 3102017jc01001).

Reference

1 Wulff A & Sarhan G, *Angew Chemie Int Edn. English*, 11 (1972) 334.
2 Xing R, Ma Y, Wang Y, Wen Y & Liu Z, *Chem Sci*, 10 (2019) 1831.
3 Ansari S & Masoum S, *Anal Chem*, 114 (2019) 29.
4 Luo J, Huang J, Cong J J, Wei W & Liu X Y, *ACS Appl Mater Interfaces*, 9 (2017) 7735.
5 Zhao Y J, Chen Y J, Fang M Y, Tian Y B, Bai G Y & Zhuo K L, *Anal Bioanal Chem*, 412 (2020) 5811.
6 Dabrowski M, Ziminska A, Kalecki J, Cieplak M, Lisowski W, Maksym R, Shao S, D'Souza F, Kuhn A & Sharma P S, *ACS Appl Mater Interfaces*, 11 (2019) 9265.
7 Hoshino Y, Koide H, Urakami T, Kanazawa H, Kodama T, Oku N & Shea K J, *J Am Chem Soc*, 132 (2010) 6644.
8 Yang H, Li L, Ding Y, Ye D, Wang Y, Cui S & Liao L, *Biosens Bioelectron*, 92 (2017) 748.
9 Zaidi S A, *Drug Deliv*, 23 (2016) 2262.
10 Chen L, Xu S & Li J, *Chem Soc Rev*, 40 (2011) 2922.
11 Li X, Zhou J, Tian L, Wang Y, Zhang B, Zhang H & Zhang Q, *Sensor Actuat B-Chem*, 241 (2017) 413.
12 Zuoting Yang, Junjie Chen, Ke Yang, Qiuyu Zhang & Baoliang Zhang, *J Colloid Interface Sci*, 570 (2020) 182.
13 Ali Jahanban-Esfahlan, Leila Roufegarinejad, Rana Jahanban-Esfahlan, Mahnaz Tabibiazar & Ryszard Amarowiczh, *Talanta*, 207 (2020) 120317.
14 Kaiguang Yang, Senwu Li, Jianxi Liu, Lukuan Liu, Lihua Zhang & Yukui Zhang, *Anal Chem*, 88 (2016) 5621.
15 Shiting Zhang, Zhiqiang Liu,Siyu Jin, Yufei Bai, Xingjia Feng & Guoqi Fu, *Talanta*, 234 (2021) 122690.
16 Zhou J, Wang Y, Ma Y, Zhang B & Zhang Q, *Appl Surf Sci*, 486 (2019) 265.
17 Lishuang Wang & Longshan Zhao, *Colloids Surfaces A: Physicochem Eng Asp*, 632 (2022) 127843.
18 Ertürk G, Berillo D, Hedström M & Mattiasson B, *Biotechnol Rep*, 3 (2014) 65.
19 Xia J, Cao X, Wang Z, Yang, M Zhang F, Lu B, Li F, Xia L, Li Y & Xia Y, *Sens Actuators B Chem*, 225 (2016) 305.
20 Ohno Y, Maehashi K, Yamashiro Y & Matsumoto K, *Nano Lett*, 9 (2009) 3318.
21 Murugan E, Rani D P G, Srinivasan K & Muthumary J, *Expert Opin Drug Deliv*, 10 (2013) 1319.
22 Yogaraj V, Gowtham G, Akshata C R, Manikandan R, Murugan E & Arumugam M, *J Drug Deliv Sci Technol*, 58 (2020) 101785.
23 Murugan E, Rani D P G & Yogaraj V, *Colloids Surfaces B Biointerfaces*, 114 (2014) 121.
24 Murugan E, Akshata C R, Yogaraj V, Sudhandiran G & Babu D, *Ceram Int*, 48 (2022) 16000.
25 Murugan E, Yogaraj V, Rani D P G & Sinha A K, *RSC Adv*, 5 (2015) 106461.
26 Yilin Wu, Li Chen, Tongfan Hao, Jian Lu, Jia Gao, Xinyu Lin, Jiuyun Cui, Chunxiang Li & Yongsheng Yan, *J Colloid Interface Sci*, 531 (2018) 1.
27 Chen H J, Zhang Z H & Luo L J, *Senso Actuat B: Chem*, 163 (2012) 76.
28 Deng Z, Zhen Z & Hu X, *Biomaterials*, 32 (2011) 4976.
29 Liu Y, Chen M M & Song L, *J Luminescence*, 134 (2013) 515.
30 Chen H, Kong J & Yuan D, *Biosens Bioelectron*, 53 (2014) 5.
31 El-Sharif H F, Yapati H & Kalluru S, *Acta Biomater*, 28 (2015) 121.
32 Liu M, Pi J & Wang X, *Analytica Chimica Acta*, 932 (2016) 29.
33 Qin L, He X W & Zhang W, *Anal Chem*, 81 (2009) 7206.
34 Li W, Sun Y & Yang C, *JACS Appl Mater Interfaces*, 7 (2015) 27188.
35 Dong X, Ma Y & Hou C, *Polym Int*, 2019 (2019) 955.
36 Xu J, Prost E & Haupt K, *Sens Actuat B: Chem*, 258 (2018) 10.
37 Li W, Sun Y & Yang C, *JACS Appl Mater Interfaces*, 7 (2015) 27188.
38 Wang P, Zhu H & Liu J, *Chem Eng J*, 358 (2019) 143.
39 Li X, Zhang B & Li W, *Biosens Bioelectron*, 51 (2014) 261.
40 Zhou J, Wang Y & Ma Y, *Appl Surf Sci*, 486 (2019) 265.
41 Wang Y, Zhou J & Zhang B, *Chem Eng J*, 327 (2017) 932.
42 El-Sharif H F, Yapati H, Kalluru S & Reddy S M, *Acta Biomaterialia*, 28 (2015) 121.
43 Huachang Chen, Juan Kong, Dongying Yuan & Guoqi Fu, *Biosens Bioelectron*, 53 (2014) 5.
44 Xiajuan Zou, Dan Liu, Lijun Zhong, Bin Yang, Yaxin Lou, Baihe Hu & Yuxin Yin, *Anal Bioanal Chem*, 401 (2011) 1251.
45 Wang S, Yang L, Cho H Y, Dean Chueng S T, Zhang H, Zhang Q & Lee K B, *Biomaterials*, 224 (2019) 119498.
46 Wang S, Zheng H, Zhou L, Cheng F, Liu Z, Zhang H, Wang L & Zhang Q, *Nano Lett*, 20 (2020) 5149.
47 Xu J, Prost E & Haupt K, *Sens Actuat B: Chem*, 258 (2018) 10.
48 Wang P, Zhu H & Liu J, *Chem Eng J*, 358 (2019) 143.
49 Zheng J, Lin Z & Lin G, *J Mater Chem B*, 3 (2015) 2185.
50 Wu J, Luan M & Zhao J, *J Biol Macromol*, 39 (2006) 185.